AD_____

Award Number: W81XWH-13-2-0036

TITLE: Pre-clinical and Clinical Development of Low Dose Methamphetamine for the Treatment of Traumatic Brain Injury

PRINCIPAL INVESTIGATOR: David Poulsen, PhD

CONTRACTING ORGANIZATION: University of Montana, Missoula, MT 59812

REPORT DATE: Dec 2014

TYPE OF REPORT: Final

PREPARED FOR: U.S. Army Medical Research and Materiel Command
Fort Detrick, Maryland 21702-5012

REPORT DOCUMENTATION PAGE

Form Approved
OMB No. 0704-0188

1. REPORT DATE	2. REPORT TYPE	3. DATES COVERED
December 2014	Final	April 1, 2013-Sept 30, 2014

4. TITLE AND SUBTITLE
Pre-clinical and Clinical Development of Low Dose Methamphetamine for the Treatment of Traumatic Brain Injury

5a. CONTRACT NUMBER

5b. GRANT NUMBER
W81XWH-13-2-0036

5c. PROGRAM ELEMENT NUMBER

6. AUTHOR(S)
David Poulsen

E-Mail: david.poulsen@umontana.edu

5d. PROJECT NUMBER

5e. TASK NUMBER

5f. WORK UNIT NUMBER

7. PERFORMING ORGANIZATION NAME(S) AND ADDRESS(ES)

University of Montana
32 Campus Dr.
Missoula, MT 59812

8. PERFORMING ORGANIZATION REPORT NUMBER

9. SPONSORING / MONITORING AGENCY NAME(S) AND ADDRESS(ES)
U.S. Army Medical Research and Materiel Command
Fort Detrick, Maryland 21702-5012

10. SPONSOR/MONITOR'S ACRONYM(S)

11. SPONSOR/MONITOR'S REPORT NUMBER(S)

12. DISTRIBUTION / AVAILABILITY STATEMENT
Approved for Public Release; Distribution Unlimited

13. SUPPLEMENTARY NOTES

14. ABSTRACT
This proposal addresses additional preclinical characterization of low dose methamphetamine as a neuroprotective agent for TBI. We have previously demonstrated that treatment with methamphetamine within 12 hours after TBI significantly improved cognition and functional behavior in 2-3 month old male Wistar rats. These studies were intended to examine the therapeutic effects of methamphetamine in female and aged male rats. We also repeated a MRI time course study with the intent of determining if there was a dose response effect associated with methamphetamine induced white matter track remodeling. We have determined that female rats represent a poor model for TBI. Unlike humans, female rats have a 3-day estrous cycle. This means they are endogenously exposed to the neuroprotective effects of estrogen and progesterone before, during and after injury. This allows them to recover to near normal levels within a few weeks of after injury. In this context, it is not possible to observe any kind of drug effect on cognitive or behavioral outcomes. We have determined that methamphetamine does not exhibit a therapeutic effect in aged rats. A number of changes exist in aged rats that could account for this observation. First, they have reduced dopamine receptors. We have shown that methamphetamine-mediated neuroprotection is dependent, in part, on the activation of dopamine receptors. This reduction of dopamine receptors also contributes to a condition of chronic inflammation. We have shown that methamphetamine reduces neuroinlammatory signaling. Thus, the reduction of dopamine receptor mediated signaling could explain the loss of protective effect in aged rats. The MRI time course series confirmed our previous results but we did not observe a dose response effect. However, we did determine that methamphetamine treatment significantly increased neurovascular staining in the perilesional region. This diata suggests that methamphetamine treatment also enhances angiogenesis after injury.

15. SUBJECT TERMS nothing listed

16. SECURITY CLASSIFICATION OF:			17. LIMITATION OF ABSTRACT	18. NUMBER OF PAGES	19a. NAME OF RESPONSIBLE PERSON
a. REPORT	b. ABSTRACT	c. THIS PAGE			USAMRMC
U	U	U	UU	24	19b. TELEPHONE NUMBER *(include area code)*

Table of Contents

Page

INTRODUCTION

We have previously demonstrated that treatment with low dose methamphetamine results in significant improvements in cognition, functional behavior (Rau et al., 2012, 2014). We have also demonstrated that methamphetamine treatment significantly preserved axons, dendrites and enhanced white matter track remodeling in the perilesional region following severe TBI (Ding et al., 2013). Finally, we recently demonstrated that methamphetamine treatment significantly reduces seizure susceptibility following severe TBI. The purposes of the currant studies are: 1) to investigate the potential therapeutic effects of methamphetamine on female and aged male rats; 2) to investigate the dose response effects of methamphetamine on white matter track remodeling; and 3) to submit an amended IND application to FDA in preparation for a phase IIA dose escalation safety study. The aged and female studies were proposed in an effort to be compliant with recent recommendations

KEY WORDS

Traumatic brain injury, neuroprotection, methamphetamine, aged rats, female rats, MRI, neurological severity score, foot fault, Morris water maze, confidential investigator brochure, investigational new drug application.

OVERALL PROJECT SUMMARY

Aim 1: Test the hypothesis that low dose methamphetamine is neuroprotective when administered to aged or female rats after severe TBI.

We used the lateral fluid percussion injury model to induce severe TBI in 10-12 month old male Wistar rats. Rats were treated with a bolus IV injection of 0.4 mg/kg methamphetamine followed by continuous IV infusion with 0.5mg/kg/hr methamphetamine for 24 hours. Control rats received the same injection and infusion but with saline. Only rats with a severe TBI (neurological severity score of 10 or higher) were used. Functional behavior was assessed in all rats based on neurological severity scores (NSS) and foot fault assessments on day-1 post injury and then again weekly for 5 weeks. As figure 1 indicates, there was a significant difference in both the NSS and foot fault outcomes between uninjured sham rats and TBI injured rats. However, unlike the young rats, methamphetamine did not induce a significant improvement in for behavioral outcomes (NSS or foot fault) in the aged rats over the 5-week test period. These data suggest that methamphetamine is not neuroprotective in aged Wistar rats.

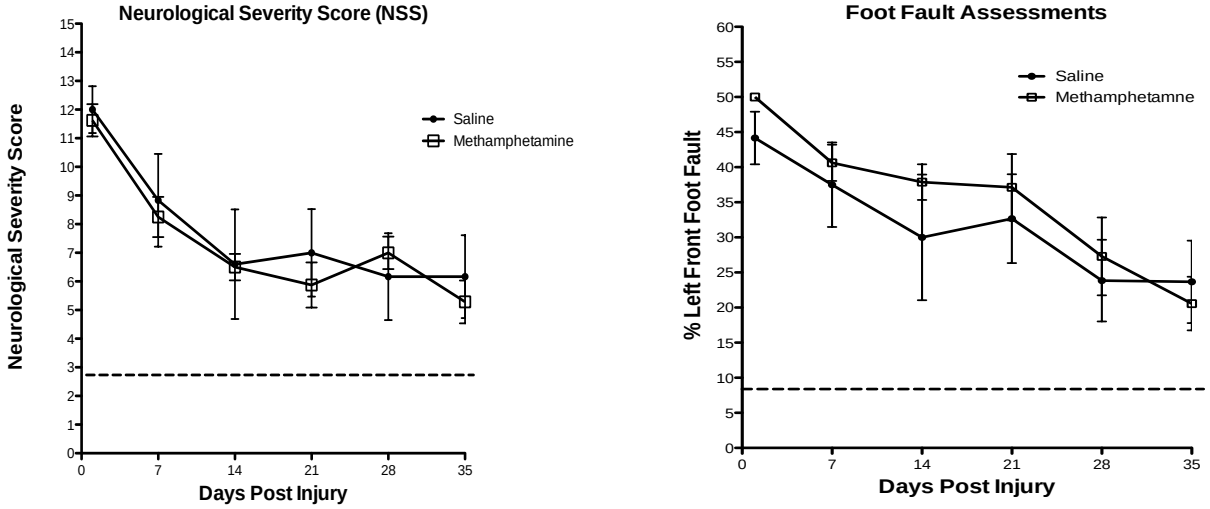

Figure 1. Methamphetamine does not improve behavioral outcomes in aged rats after severe TBI. Unlike younger rats (2-3 months old), there were no significant differences observed between saline and methamphetamine treated aged rats with either of the behavioral outcome measures tested. The dashed line indicates the average score observed for uninjured, sham-operated control rats. The significant difference between sham controls and TBI rats indicates an injury effect and that NSS and foot fault are appropriate outcome measures.

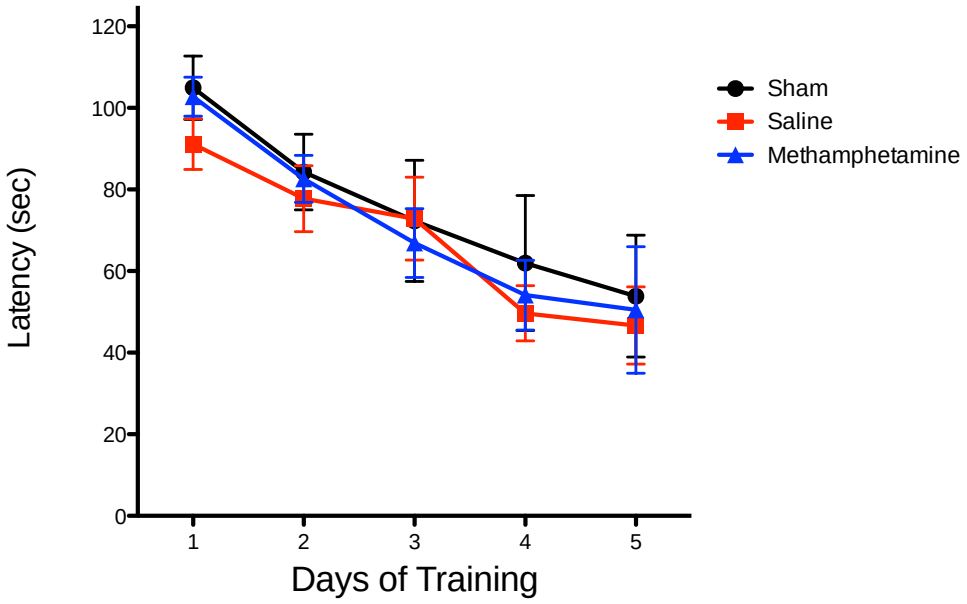

Figure 2. No significant differences in learning ability were observed between sham, saline or methamphetamine treated rats in the Morris water maze. Latency (time to locate submerged escape platform) is shown for sham (black), saline (red) and methamphetamine (blue) treated rats.

We further tested the potential of methamphetamine to improve cognition in aged rats similar to what we saw in younger rats (Rau et al., 2012, 2014). At 6 weeks post injury/treatment all rats were trained for 5 days in the Morris water maze. Each rats received four training sessions/day. The time each rat took to learn the location of a submerged escape platform (latency) was recorded. Figure 2 shows the average latency times for rats in each treatment group on each of the five training days. Even the uninjured, aged rats showed significant learning impairment relative to latency times we previously observed for young rats. Due to the poor performance of the aged sham controls in the Morris water maze, it was not possible to detect a difference due to injury and therefore impossible to detect a difference due to a drug effect.

As mentioned above, methamphetamine mediates neuroprotection in part, through the activation of dopamine receptors. Its been shown that aged rats and humans have reduced expression of dopamine receptors. Therefore, we reasoned that increasing the dose in aged rats might be required to see a therapeutic effect. The first group of aged rats received a bolus injection plus IV infusion with 0.5 mg/kg/hr for 24 hours. Therefore, we tested a dose of 1.0 mg/kg/hr in a second cohort. Five aged, male, Wistar rats were treated at this higher dose. All five rats died within the 24-hour dosing period. Given this high rate of mortality we did not feel that it was ethical or of scientific value to continue and include additional animals. Given this observation, we reevaluated the doses administered and compared the absolute dose given versus the dose/weight administered to young and aged rats. This seemed relevant due to the fact that the aged rats were substantially heavier (average weight = 576 $\pm$ 59g) compared to the younger rats (average weight = 377 $\pm$ 45g). As a consequence, the average absolute total dose of methamphetamine previously given to young rats was 4.68 mg. In contrast, the average absolute total dose given to the first cohort of aged rats was 7.15 mg. This represents 1.5 times the absolute dose given to younger rats. Furthermore, the second aged cohort, that experienced 100% mortality, was given an average absolute total dose of 13.85 mg. Thus, the average absolute total dose given to the second aged cohort was almost three times higher than the dose given to the young rats.

We next examined the neuroprotective potential of methamphetamine following a severe TBI in young (2-3 months old), female, Wistar rats. Again, only rats that scored 10 or higher on the NSS assessment at 24 hours after injury were included in these studies. This insured that all rats received a similar injury of sufficient severity. Behavioral assessments (NSS and foot fault) were conducted on all rats on a weekly basis for five

weeks post-injury. As Figure 3 indicates, there were no significant differences in either NSS or foot fault assessment scores during the testing period.

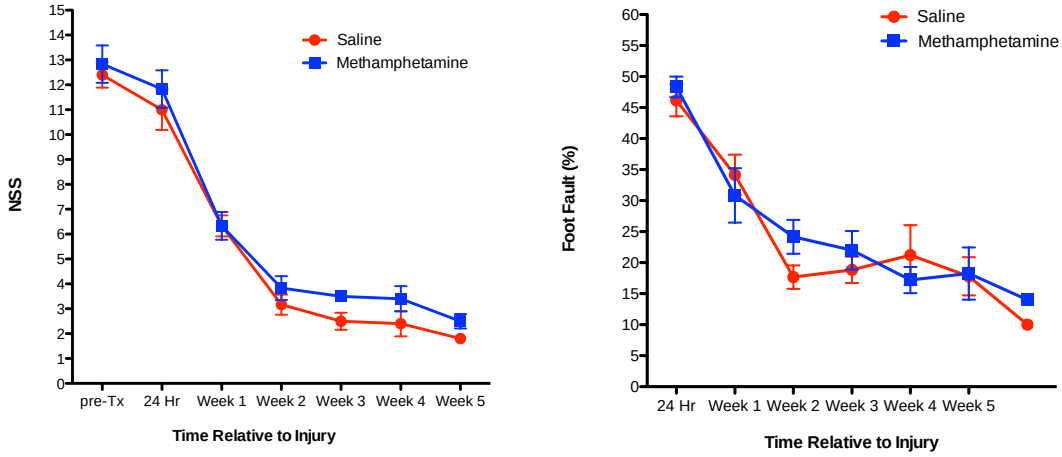

Figure 3. Methamphetamine does not induce a significant improvement in female rats after severe TBI. NSS (left panel) and Foot Fault (right panel) assessments over a 5 week time course following severe TBI are shown for saline (red) and methamphetamine (blue) treated rats.

We previously demonstrated that methamphetamine treatment significantly improved cognitive outcomes following severe TBI in young, male Wistar rats. Therefore, we wanted to further examine the potential of methamphetamine to improve cognitive function in female rats. Interestingly, unlike the behavioral assessments, saline treated TBI control rats did exhibit impairment in the Morris water maze one month after injury (Figure 4). Unfortunately, although the data suggested that methamphetamine treatment caused a trend toward improvement, a significant difference from saline treated controls was not observed.

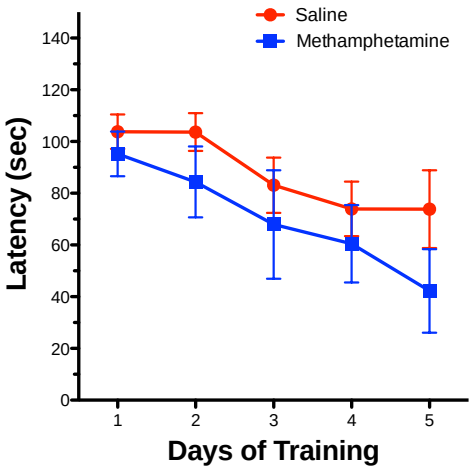

Figure 4. Cognitive testing of female Wistar rats after severe TBI. Female rats were tested in the Morris water maze 30 days after receiving a severe TBI. Latency (time to locate escape platform) over 5 training days is shown for rats treated with saline (red) or methamphetamine (blue) following severe TBI.

Aim 2: Test the hypothesis that low dose methamphetamine can improve neurovascular changes and axonal remodeling over time.

MRI measurements after TBI with and without Methamphetamine treatment: MRI measurements were performed one day before TBI, 1 and 3 days post TBI (using the controlled cortical impact model), and then weekly for 6 weeks. MRI studies were performed using T1, T2, T2*, and fractional anisotropy (FA). Stereotactic ear bars were used to minimize movement during the imaging procedure. During MRI measurements, anesthesia was maintained using a gas mixture of N_2O (69%), O_2 (30%) and isoflurane (1-1.5%). Rectal temperature will be maintained at 37°C using a feedback controlled water bath. After the last MRI measurements, the animals were sacrificed. White matter changes in the brain tissue were assessed by specific immuno-histochemical staining. The analyzed data were obtained from ten control and eight treated animals.

T_2 measurement: T_2 was measured using a Carr-Purcell-Meiboom-Gill multislice multiecho (six echo) MRI. A series of four sets of images (13 slices for each set) were obtained using TEs of 15, 30, 45, 60, 75, and 90 msec and a TR of 4.5 sec. Images were produced using a 32 mm FOV, 1 mm slice thickness, 128 x 128 image matrix.

T_2^* measurement: T_2^* was obtained using a gradient echo multislice multiecho sequence. A TR value of 4.5 sec was used with echo times of 3.5, 15, 20, 25, 30, and 35 msec. Images were produced with a 32mm FOV, 1mm slice thickness, 13 slices, and 128 X 128 image matrix.

***Diffusion Tensor MRI (DTI) measurement*:** DTI was acquired using pulsed gradient spin-echo echo-planar (EPI) sequence with echo-planar readout. The field of view was 32 mm; two average, 128x128 imaging matrix, 1 mm slice thickness with 13 slices, TR = 800 ms and TE = 36 ms, 16 shots, 4 averages, 15 diffusion attenuate weighted images with b = 1200, 600, and 0 s/mm^2 in each slice.

***MRI ANALYSIS*:** The TBI lesion was identified on the MRI T_2 map. The lesion area on each slice of T_2 map was specified by those pixels with a T_2 value higher than the mean plus twice the standard deviation (mean + 2SD) measurements provided by the normal tissue on the pre-TBI T_2 map. Lesion volume was obtained by adding all the areas measured on individual slices and multiplying each area by the slice thickness.

The volume of the lateral ventricle was measured on T_2 maps at a fixed structural location presented by six contiguous coronal T_2 slices using similar criterion as described above to identify the ventricular area on each slice. The ventricular volume was obtained by adding all the areas measured on individual slices and multiplying each area by the slice thickness. The ventricle volumes measured at various time points were normalized for each animal to the ventricular volumes measured at pre-TBI.

MRI regions of interest (ROI) were identified in the TBI core and recovery areas. Two ROIs were selected for analysis of MRI parameters. The first ROI, the TBI core area, was identified by using the threshold T_2 value of mean + two standard deviations from the T_2 value measured in the pre-TBI T_2 maps obtained 6 weeks after stroke. The second ROI, the TBI recovery area, was identified by subtracting the TBI core areas obtained 6 weeks after stroke from the TBI area in T_2 maps obtained 24 hours after TBI.

MRI Results:

The TBI lesion volumes were measured using T_2 maps at 24 hours, and weekly from 1 to 6 weeks post-TBI and normalized to the lesion volume obtained 24 hours after TBI. There was a marginal transient reduction of normalized lesion volume at 3 days (p=0.055) after TBI. However, there was no treatment effect on the normalized TBI lesion volume compared to controls with the analyzed data (Figure 5).

Figure 5

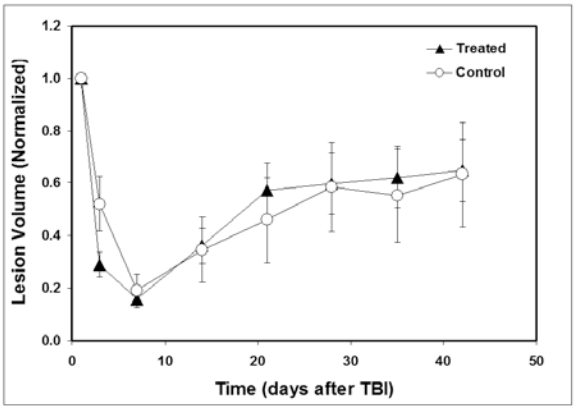

The relative ventricular volumes were measured using T_2 maps before TBI, and at 24 hours, and weekly from 1 to 6 weeks post-TBI and normalized to the ventricular volume obtained before TBI. There was no treatment effect on normalized ventricular volume compared to controls (Figure 6).

Measurements of T_2 and T_2^* were performed on the TBI core and recovery ROIs (perilesional region). The relative changes of MRI measurements in the TBI core ROI (TBI core/Pre-TBI core) and recovery ROI (TBI recovery/Pre-TBI recovery) were calculated and used in the analysis. There was no treatment effect on the TBI relative T_2 and T_2^*, compared to controls with the analyzed data.

Figure 6

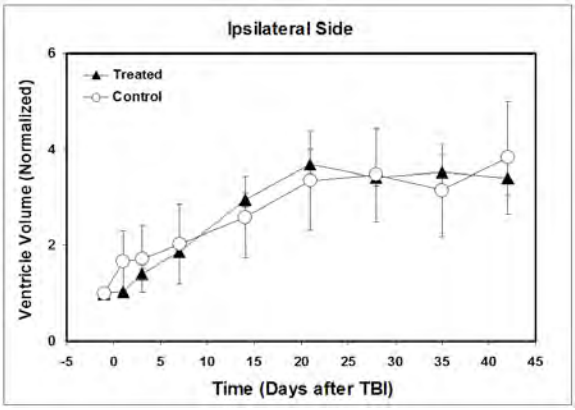

A

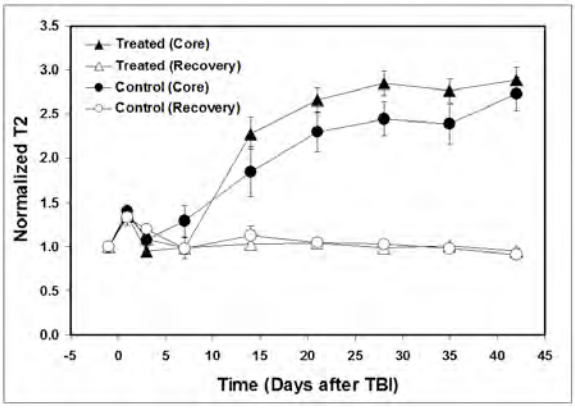

B

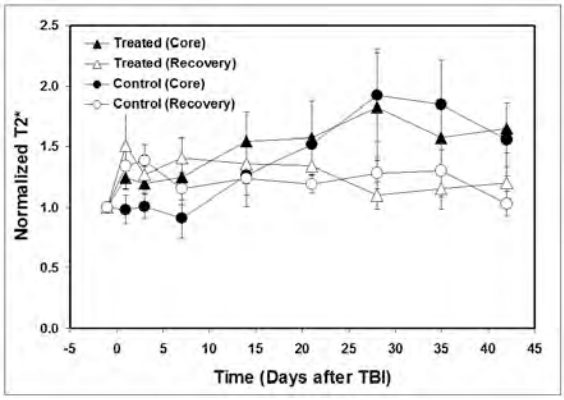

Figure 7. T2 (A) and T2* (B) image analysis of the injury core (filled symbols) and perilesional region (open symbols) for saline treated (circles) and methamphetamine treated (triangles) rats. Time course shown is days after TBI.

Measurements of FA were performed on the TBI core and recovery ROIs to determine white matter track remodeling. The relative changes of FA ($FA_{post\_TBI}/FA_{pre\_TBI}$) in the TBI injury core and recovery ROI (perilesional region) were calculated and used in the analysis. The methamphetamine treated group revealed large increases in FA in the TBI recovery regions compared with the saline treated control group, and significant differences in FA were detected at 5 (p=0.020) and 6 (p=0.017) weeks after TBI (Figure 8). There were no significant differences in FA in the TBI core regions between treated and control groups.

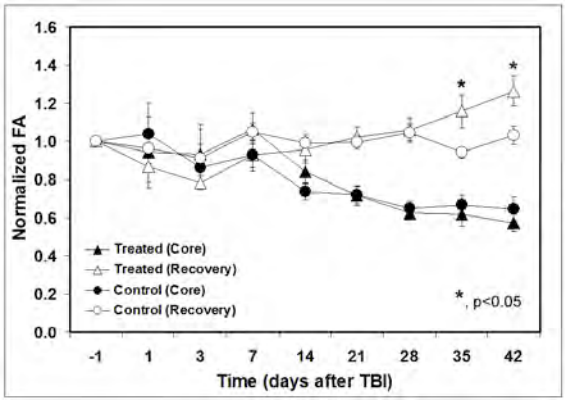

Figure 8. T2 (A) and T2* (B) image analysis of the injury core (filled symbols) and perilesional region (open symbols) for saline treated (circles) and methamphetamine treated (triangles) rats. Time course shown is days after TBI.

***Immunohistochemistry staining*:** At 42 days after TBI, rats were anesthetized intraperitoneally with chloral hydrate, and perfused transcardially with saline, followed by 4% paraformaldehyde. Brains were isolated, post-fixed in 4% paraformaldehyde for 2 days at room temperature, and then processed for paraffin sectioning. Using light microscopy and laser scanning confocal microscopy (LSCM), we measured a composite index of independent measurements of axon, microvessel, dendrite, synapse immuno-histochemistry (Bielshowsky /fast blue, EBA, SMI-310, SMI-32, MAP-2 and synaptophysin) and lesion volume.

Neurobehavioral functional tests: Neurological function was monitored by modified neurological severity scores (mNSS) and foot-fault test. Baseline neurological function was established for all animals prior to TBI and again on days 1, 7, 14, 21, 28, 35, and 42-post injury. On day 38 to day 42, the Morris Water Maze (MWM) test was performed to assess the impact of methamphetamine on cognitive function (learning and memory) following TBI.

Histopathology (CCI model):

Bielschowsky and Luxol fast blue labeled axons and myelin, respectively, and were used to monitor changes in cerebral white matter in the TBI boundary ROI (perilesional region). Significant increases ($p<0.034$) in Bielschowsky and Luxol Fast Blue staining area in the TBI boundary ROI were detected in the methamphetamine treated group (35.5±19.8) compared with the control group (17.6±3.0) (Figure 9). Likewise, a significant increase ($p<0.001$) in the number of blood vessels per mm^2 as monitored by EBA immunoreactivity was observed within the perilesional region in the methamphetamine treated group (422.4±31.5) compared to the saline treated control group (323.8±49.7) (Figure 10). In addition, significant increases were observed in dendrites labeled with MAP2 ($p<0.001$) (Figure 11), axons labeled with SMI-32 ($p=0.002$) (Figure 12), and synapses labeled with synaptophysin ($p<0.001$) (Figure 13) within the perilesional region of methamphetamine treated rats compared to the saline treated control group.

Figure 9

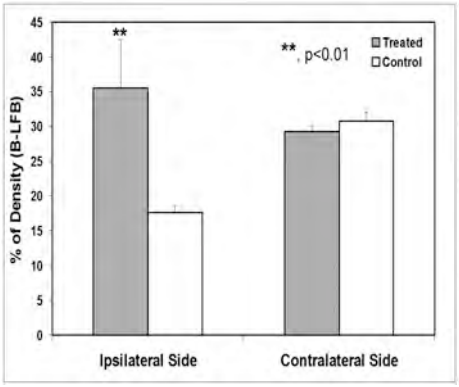

Figure 10

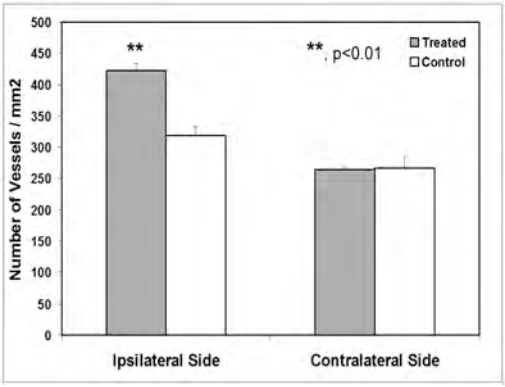

Figure 11

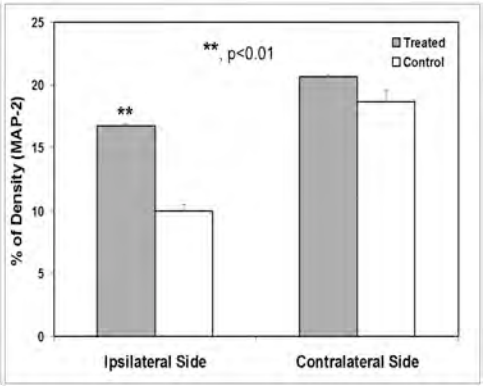

Figure 12

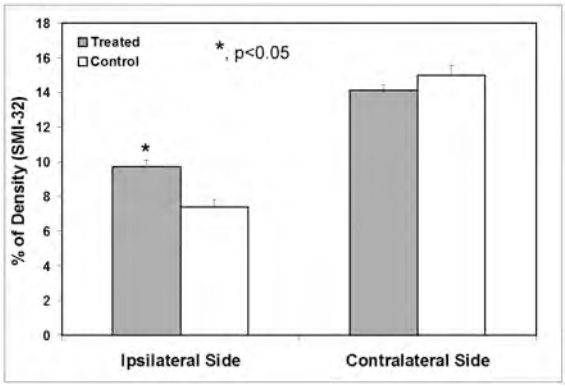

Figure 13

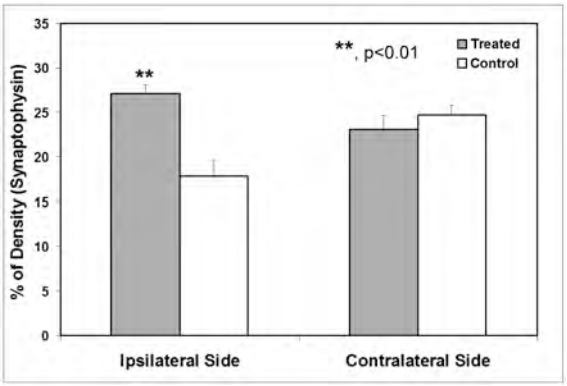

Functional behavior (CCI model)
Significant improvements in functional behavior were detected in the Methamphetamine treated group compared to the control group. Methamphetamine treated rats had significantly lower Neurological severity scores (mNSS, 1 day to 6w, $p<0.05$) and foot-fault (7 days to 4w, and 6 w $p<0.05$) tests (Figure 14).

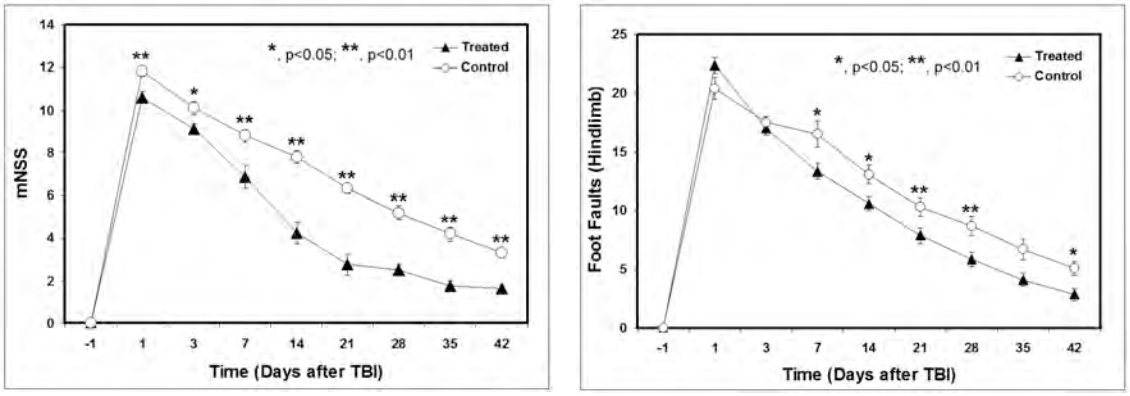

Figure 14. Methamphetamine increases functional behavior following severe TBI in CCI model. Serial mNSS (left panel) and foot fault assessments (right panel) are shown for methamphetamine treated (dark triangles) and saline treated controls (open circles).

In summary, low dose (a bolus injection of 0.4mg/kg followed by an infusion of 0.5mg/kg/hr for 24 hrs) methamphetamine treatment starting at 8 hours after TBI in rats significantly improved the recovery of behavioral functions in rats by lowering mNSS and foot-fault scores after TBI, compared with saline treatment. The treatment promoted neurological recovery after TBI, which was detected by MRI measurement of FA and confirmed by immunohistochemical outcomes. The increased FA, indicating a more reorganized white matter, may contribute to the functional recovery after TBI in rats.

Aim 3: Secure FDA approval of a phase I/II clinical trial plan and obtain an amended IND in preparation for initiating human clinical testing in TBI patients.

We have received correspondence from Dr. Russell Katz, M.D., (Director of the Division of Neurology Products, CDER), in which the FDA has requested toxicity studies in rats and dogs be completed before an amended IND and additional clinical trials can be approved. This request is consistent with the FDAs guidance for industry regarding nonclinical evaluation of reformulated drug products intended for administration by a route that is different from the currently approved formulation. Methamphetamine is currently FDA approved for oral administration. Therefore, the administration of an IV formulation, as we are proposing, necessitates the additional toxicity studies requested by the FDA. The FDA Guidance for Industry: *M3(R2) Non Clinical Safety Studies for the Conduct of Human Clinical Trials and Marketing Authorization for Pharmaceutical*, also recommends that safety pharmacology studies be conducted as well. Given the potential for methamphetamine to induce abnormal cardiac rhythms at higher doses, we also feel that it is prudent to conduct a cardiovascular safety pharmacology study in dogs. The completion of the proposed preclinical toxicity and safety studies, combined with the long clinical history and safe use of methamphetamine at low doses, will provide a well defined, safe dose range for testing in a phase IIA dose escalation safety study in TBI patients. A JWMRP proposal has been submitted and we hope this support will become available to complete these studies. Without the completion of these toxicity studies it will not be possible to complete this aim.

Aim 4: Prepare a confidential investigator brochure (CIB) to support the submission of an amended IND application to the FDA.

Draft of the final FDA reports that are to be included in the CIB are currently being completed.

Key Research Accomplishments

- We have determined that methamphetamine does not induce significant improvements in functional behavior or cognition in aged rats following severe TBI in the LFP injury model.
- We have determined that NSS and foot fault assessments represent very poor outcome measures in female rats following a severe TBI in the LFP model.
- We have demonstrated that methamphetamine treatment does not produce a significant improvement in cognition in female rats following severe TBI with the LFP model.
- We have shown that methamphetamine treatment significantly improves white matter track remodeling, preserves axons, dendrites and synapses within the perilesional region following severe TBI in the CCI model.
- We have shown that methamphetamine treatment significantly improves labeling of blood vessels within the perilesional region following severe TBI in the CCI model.

Efforts under EWOF (April 1-Sept 30, 2014)

To further extend the observations of Aim 3 and better understand the potential molecular mechanisms of methamphetamine-mediated neuroprotection, we conducted additional histological analysis of brain tissues collected from Control rats, as well as TBI injured rats treated with either saline or low dose methamphetamine.

First, we have previously reported that treatment with low-dose methamphetamine reduced the gene expression of pro-inflammatory signals, such as interleukin-1β and MYD88, while significantly increasing the expression of the anti-inflammatory chemokine CXCL12 following TBI (Rau et al, 2014). Microglia play a critical role in neuroinflammation. Therefore, we hypothesized that low dose methamphetamine may mediate neuroprotection in part by modulating microglial activation. To test this hypothesis we chose to focus on labeling total microglia with antibodies directed against ionized calcium-binding adaptor molecule 1 (Iba1) and phagocytic microglia with antibodies directed against Cluster of Differentiation 68 (CD68). However, it is important to note that these markers do not differentiate between resident microglia and infiltrating macrophages (Hernandez-Ontiveros et al, 2013). Using these approaches we monitored region-specific microglial activation between 48 hours and two weeks post injury.

Within two weeks after TBI, an increase in both phagocytic ($CD68^+$) and non-phagocytic ($CD68^-$) $Iba1^+$ microglia was observed in the cortex, corpus callosum, dentate gyrus, CA3 radiatum, fimbria and thalamus. However, temporal and spatial differences were observed in both Iba1 and CD68 labeling. Although the cortex receives the brunt of the TBI itself, there was not a significant increase of activated microglia at 48 hours after injury (Figure 15). In contrast, increased labeling of Iba1 within the cortex was observed one week after TBI and remained elevated at the two-week time point. Interestingly, CD68 labeling did not parallel the increase of Iba1 labeling seen at one and two weeks post-TBI.

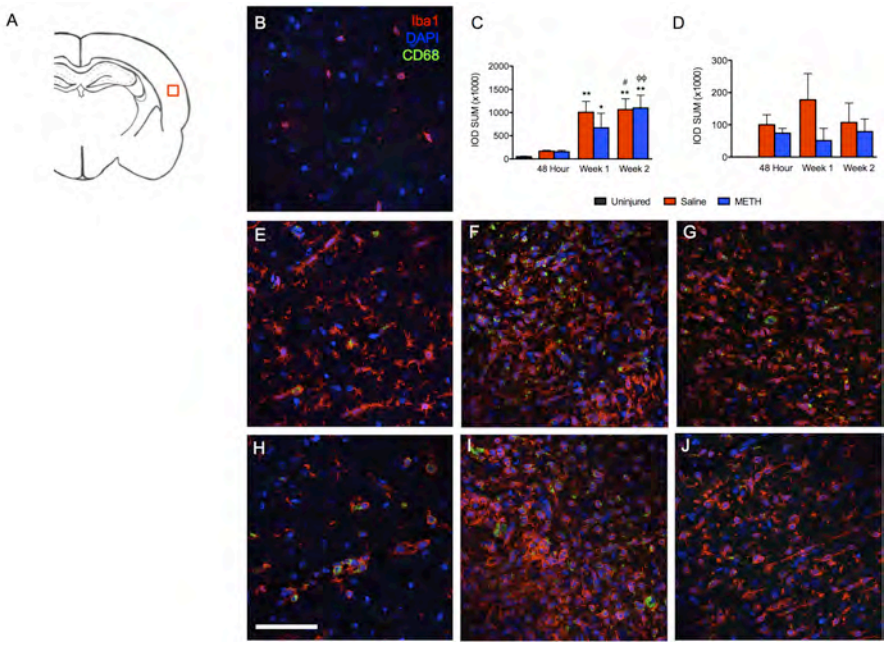

Figure 15: Microglia are activated in the cortex core injury at 1 and 2 weeks post-TBI. Iba1 (red), CD68 (green) and DAPI (blue). (A) Schematic of a rat brain at Bregma -3.3 with red box marking location of analysis, (B) Uninjured, (C) Summary graph of Iba1, (D) Summary graph of CD68, (E) Saline at 48 hours, (F) Saline 1 week after TBI, (G) Saline 2 weeks after TBI, (H) Methamphetamine at 48 hours post-TBI, (I) Methamphetamine one week post-TBI, and (J) Methamphetamine 2 weeks post-TBI. 48 hours (Saline n=6; Methamphetamine n=6), 1 Week (Saline n=5; Methamphetamine n=4), 2 Weeks (Saline n=4; Methamphetamine n=40), * = $p<0.05$ compared to uninjured, ** = $p<0.01$ compared to uninjured; # = $p<0.05$ compared to 48 hour Saline, and ϕϕ = $p<0.01$ compared to 48 hour Methamphetamine; scale bar = 80μm

In addition to amoeboid shaped microglia, we observed rod microglia within the injury zone of the cortex. Rod microglia were first observed at one week but were most evident within the cortical lesion at two weeks post-TBI. The occurrence and prevalence of rod microglia within the injury core of the cortex was not affected by treatment with methamphetamine (data not shown). Rod microglia were labeled with Iba1 but only occasionally labeled with antibodies to CD68 (Figure 16), suggesting that phagocytosis is not a consistent function of all rod microglia. Co-labeling with SMI-71 indicated that rod microglia do not align with nearby vasculature (Figure 16). Ziebell *et al* (2012; 2014) have suggested that rod microglia align with cortical axons. Indeed, staining of axons with NF312 or dendrites with MAP2, showed an undeniable alignment with rod microglia (Figure 16). Colocalization, however, was not observed with Iba1 and NF312 and only occasionally seen with Iba1 and MAP2. When colocalization was seen between MAP2 and Iba1, it consisted of the medial end of a rod cell associating with the distal tip of MAP2-labeled dendrites.

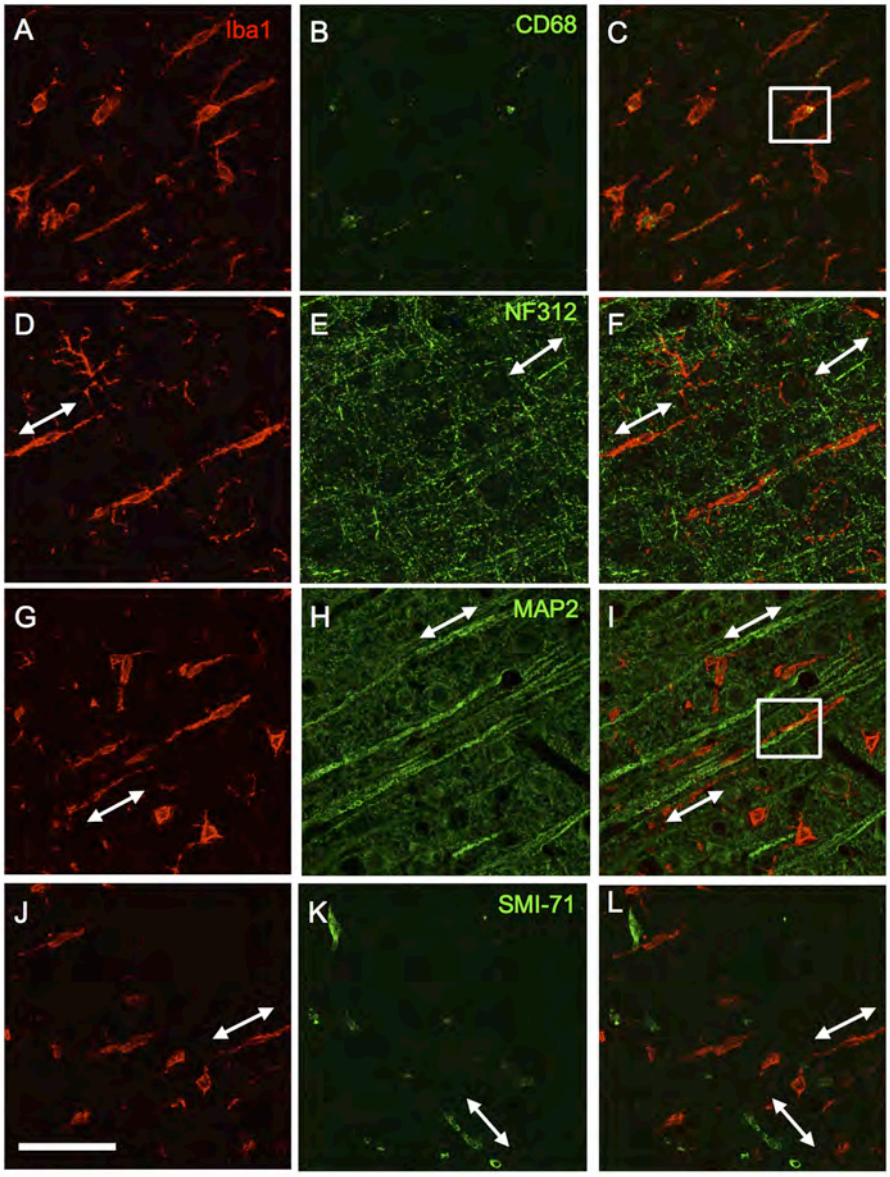

Figure 16: Rod microglia have variable phagocytic capabilities and align with neuronal axons, not blood vessels, after TBI. Images show rod microglia within the cortical core injury two weeks after TBI. The top row shows rod microglia labeled with Iba1 (A), CD68 (B) and their merged image (C). The second row shows rod microglia labeled with Iba1 (D), NF312 (E) and their merged image (F). The third row shows rod microglia labeled with Iba1 (G), MAP2 (H) and their merged image (I). The bottom row shows rod microglia labeled with Iba1 (J), SMI-71 (K) and their merged image (L). 60x images; scale bar represents 60 µm; arrows show linear direction; boxes show examples of colocalization; Iba1 (red); CD68 (green, top row); NF312 (green, second row); MAP2 (green, third row); SMI-71 (green, bottom row)

In addition to the cortex, the hippocampus often shows damage following TBI. Hippocampal sclerosis is a common consequence of TBI seen in human patients and animal models (Walker & Tesco, 2013; Xiong *et al,* 2013). Of the brain regions examined, the hippocampus showed the earliest increase in Iba1 labeling of microglia at 48 hours, with the majority of label observed within the dentate gyrus (figure 17) and the stratum radiatum of CA3 (Figure 18). In addition, there was significantly more labeling of $CD68^{+}$ microglia at 48 hours

compared to uninjured controls. The increased CD68 labeling at 48 hours was observed in both methamphetamine and saline treated rats. Interestingly, the hippocampus showed a unique pattern of Iba1/CD68 staining that differed between the treatment groups. Although a dramatic reduction in CD68 labeling was observed in both saline and methamphetamine treated rats at the one-week time point, Iba1 labeling remained significantly elevated only in the saline treated group.

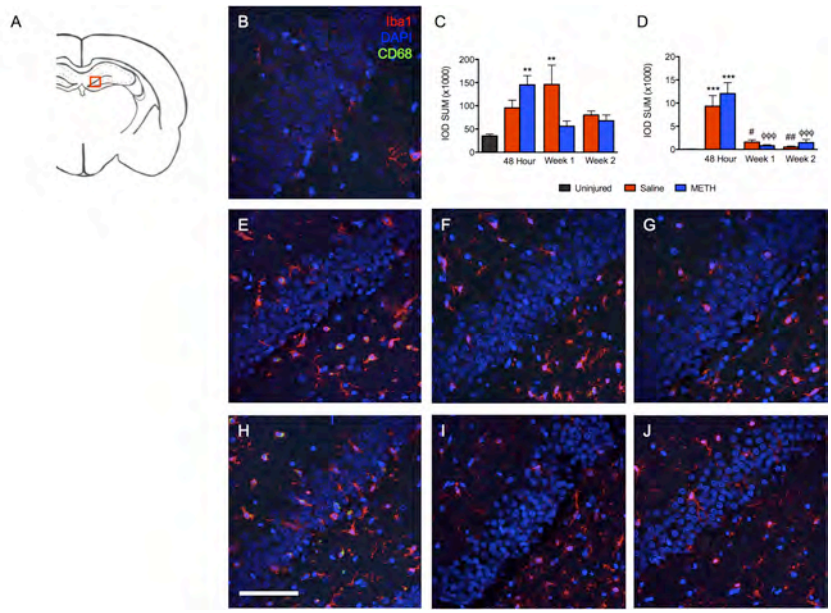

Figure 17: TBI causes increased microglia activation in the ipsilateral dentate gyrus soon after injury. Iba1 (red), CD68 (green) and DAPI (blue). (A) Schematic of a rat brain at Bregma -3.3 with red box marking location of analysis, (B) Uninjured, (C) Summary graph of Iba1, (D) Summary graph of CD68, (E) Saline at 48 hours after TBI, (F) Saline at 1 week after TBI, (G) Saline at 2 weeks after TBI, (H) Methamphetamine at 48 hours after TBI, (I) Methamphetamine at 1 week after TBI, (J) Methamphetamine at 2 weeks after TBI. 48 hours (Saline n=6; Methamphetamine n=6), 1 week (Saline n=5; Methamphetamine n=4), 2 week (Saline n=4; Methamphetamine n=4), ** = $p<0.01$ compared to uninjured, *** = $p<0.001$ compared to uninjured; # = $p<0.05$ compared to 48 hour Saline, ## = $p<0.01$ compared to 48 hour Saline and ϕϕϕ = $p<0.001$ compared to 48 hour Methamphetamine; scale bar = 80µm

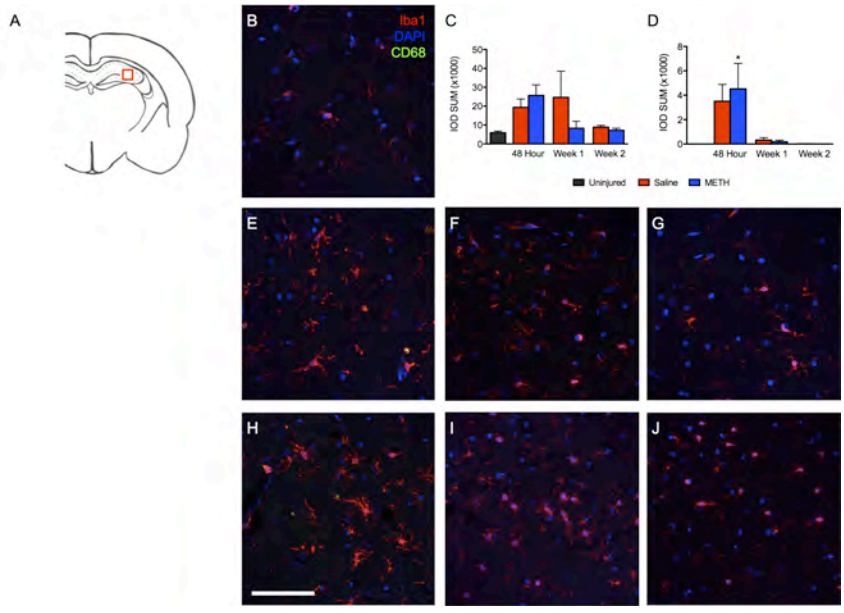

Figure 18: Microglia activation is increased in the ipsilateral CA3 stratum radiatum at 48 hours post-TBI. Images show the stratum radiatum of CA3 within the ipsilateral hippocampus labeled with Iba1 (red), CD68 (green) and DAPI (blue). (A) Schematic of a rat brain at Bregma -3.3 with red box marking location of analysis, (B) Uninjured, (C) Summary graph of Iba1, (D) Summary graph of CD68, (E) Saline at 48 hours, (F) Saline 1 week after TBI, (G) Saline 2 weeks after TBI, (H) Methamphetamine at 48 hours post-TBI, (I) Methamphetamine one week post-TBI, and (J) Methamphetamine 2 weeks post-TBI. 48 hours (Saline n=6; Methamphetamine n=6), 1 Week (Saline n=5; Methamphetamine n=4), 2 Weeks (Saline n=4; Methamphetamine n=4), * = $p<0.05$ compared to uninjured; scale bar = 80µm

Although the time course was similar between the dentate gyrus and the CA3 stratum radiatum, the magnitude of Iba1 labeling was much greater within the dentate gyrus. Further scrutiny of the microglial response within the dentate gyrus revealed a unique pattern within the granule layer. Iba1 labeling within the dentate gyrus as a whole was not different between the methamphetamine and saline treated groups. However, further analysis of the granule cell layer demonstrated a significant effect of methamphetamine treatment (Figure 19A-B). The ipsilateral granule cell layer displayed a significant increase of both Iba1 and CD68 labeling at 48 hours post-TBI; however, this response was only seen in methamphetamine-treated rats (Figure 19). Although rats treated with saline showed an increase of Iba1 within the dentate gyrus, surprisingly no increase was seen within the granule cell layer. For both treatment groups, levels of Iba1 and CD68 labeling within the granule cell layer at one and two-weeks post-TBI were approximately equivalent to those observed in uninjured animals. Since previous studies have established that the response of microglia to methamphetamine is observed bilaterally, we turned our attention to the contralateral granule layer (Thomas D., 2004). Increased Iba1 labeling was observed within the contralateral granule cell layer of methamphetamine treated TBI animals compared to saline treated and uninjured controls. Thus confirming the drug-specific effect of low-dose methamphetamine on activation of microglia within this structure (Figure 19L-Q). Interestingly, the bilateral increase of Iba1 labeling within the granule cell layer seen after methamphetamine treatment did not extend to CD68 labeling (Figure 19P). Regardless of the treatment, CD68 was only observed ipsilateral to the injury and undetectable within the contralateral dentate gyrus (Figure 19G, J, M, N). Thus, microglia showed two separate responses to two distinct stimuli, TBI and methamphetamine exposure. This dualistic response of microglia is worth investigating further and may have powerful implications for drug development. Taken together, TBI causes an increase of Iba1 and CD68 within the ipsilateral dentate gyrus regardless of treatment while treatment with methamphetamine causes a bilateral increase of Iba1 within the granule cell layer of the dentate gyrus.

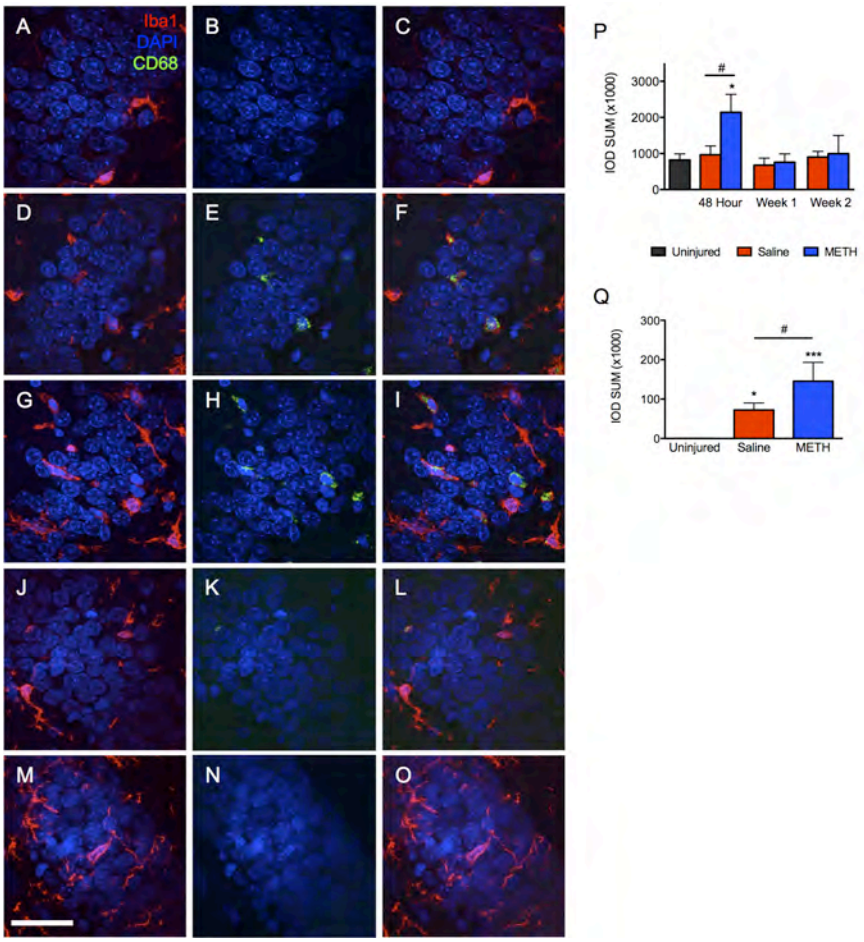

Figure 19: Methamphetamine causes a bilateral increase of microglia within the dentate gyrus granule cell layer. Images show the granule cell layer of the ipsilateral dentate gyrus at Bregma -3.3 labeled with Iba1 (red), CD68 (green) and DAPI (blue). (A) Uninjured Iba1 and DAPI, (B) Uninjured CD68 & DAPI, (C) Uninjured Iba1, CD68 and DAPI merged, (D) Saline (ipsilateral) at 48 hours post-TBI Iba1 & DAPI, (E) Saline (ipsilateral) at 48 hours post-TBI CD68 & DAPI, (F) Saline (ipsilateral) at 48 hours post-TBI Iba1, CD68, and DAPI merged, (G) Methamphetamine (ipsilateral) at 48 hours post-TBI Iba1 & DAPI, (H) Methamphetamine (ipsilateral) at 48 hours post-TBI CD68 & DAPI, (I) Methamphetamine (ipsilateral) at 48 hours post-TBI Iba1, CD68 and DAPI merged. (J) Saline (contralateral) at 48 hours post-TBI Iba1 & DAPI, (K) Saline (contralateral) at 48 hours post-TBI CD68 & DAPI, (L) Saline (contralateral) at 48 hours post-TBI Iba1, CD68, and DAPI merged, (M) Methamphetamine (contralateral) at 48 hours post-TBI Iba1 & DAPI, (N) Methamphetamine (contralateral) at 48 hours post-TBI CD68 & DAPI, (O) Methamphetamine (contralateral) at 48 hours post-TBI Iba1, CD68 and DAPI merged. (P) Summary graph of Iba1, (Q) Summary graph of CD68 seen at 48 hours post-TBI. 48 hours (Saline n=6; Methamphetamine n=6), 1 week (Saline n=5; Methamphetamine n=4), 2 week (Saline n=4; Methamphetamine n=4), 60x images, * = $p<0.05$ compared to uninjured, *** = $p<0.001$ compared to uninjured; # compared to 48 hour Saline; scale bar = 40µm

Damage to white matter tracts is a common consequence of TBI and is implicated in the development of long-term cognitive impairments. In human patients, damage to white matter tracts can be seen on scans years after a moderate or severe TBI (Adnan et al, 2013; Acosta et al, 2014; Kou & VandeVord, 2014). Furthermore, reports from both humans and animal models indicate that white matter injury (WMI) progresses temporally (Kou & VandeVord, 2014). There is also a known connection between WMI and the time course of microglia activation following TBI (Wang et al, 2013). Therefore, we investigated microglial labeling within white matter tracts in a time-dependent manner. An increase in Iba1 labeling within the fimbria ipsilateral to the injury was greatest one week after TBI in both methamphetamine and saline treatment groups (Figure 20). Both treatment groups showed a temporal pattern of CD68 labeling that mirrored total Iba1 labeling post-TBI. Both labels were significantly higher in injured rats at one-week and returned to near baseline levels by two-weeks post-TBI. In contrast, the corpus callosum, proximal to the cortical injury zone, showed the largest effect at two weeks after TBI (Figure 21). Labeling with both Iba1 and CD68 increased within the corpus callosum at each subsequent time point. Again, treatment with methamphetamine did not alter microglia activation in either the fimbria or corpus callosum at these time points.

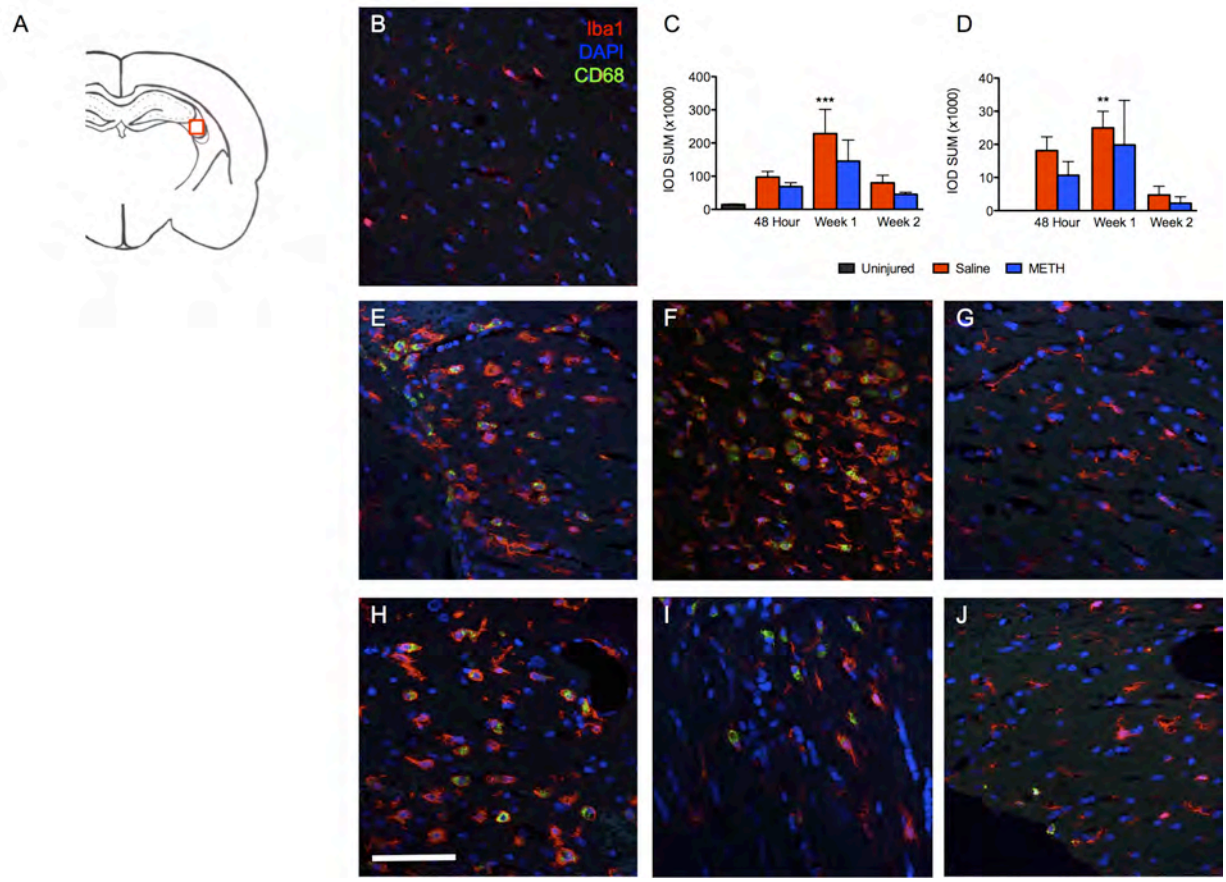

Figure 20: TBI causes increased microglia activation 1 week after injury within the ipsilateral fimbria. Images show the ipsilateral fimbria labeled with Iba1 (red), CD68 (green) and DAPI (blue). (A) Schematic of a rat brain at Bregma -3.3 with red box marking location of analysis, (B) Uninjured, (C) Summary graph of Iba1, (D) Summary graph of CD68, (E) Saline at 48 hours after TBI, (F) Saline at 1 week after TBI, (G) Saline at 2 weeks after TBI, (H) Methamphetamine at 48 hours after TBI, (I) Methamphetamine at 1 week after TBI, (J) Methamphetamine at 2 weeks after TBI. 48 hours (Saline n=6; Methamphetamine n=6), 1 week (Saline n=5; Methamphetamine n=4), 2 week (Saline n=4; Methamphetamine n=4), ** = $p<0.01$ compared to uninjured, *** = $p<0.001$; scale bar = 80µm

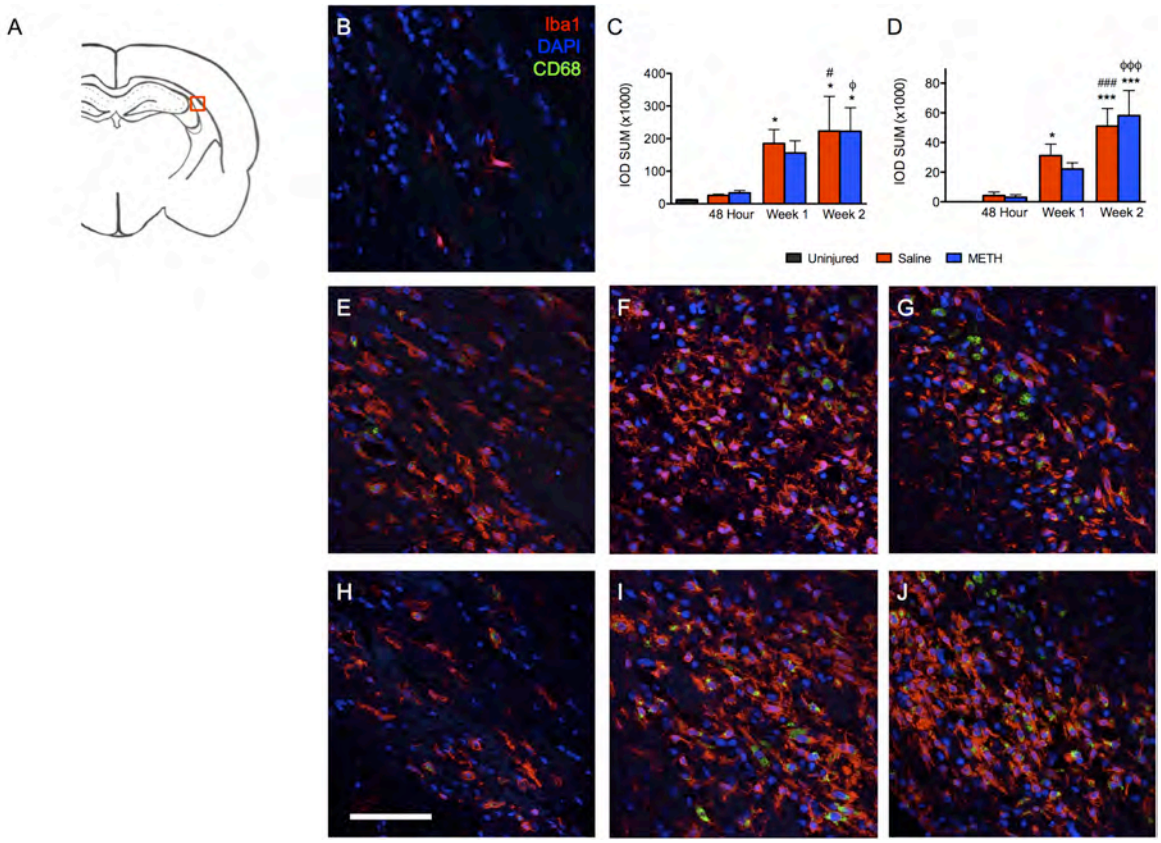

Figure 21: TBI causes a progressive increase of microglia within the ipsilateral corpus callosum. Images show the ipsilateral corpus callosum proximal to the cortical injury labeled with Iba1 (red), CD68 (green) and DAPI (blue). (A) Schematic of a rat brain at Bregma -3.3 with red box marking location of analysis, (B) Uninjured, (C) Summary graph of Iba1, (D) Summary graph of CD68, (E) Saline at 48 hours after TBI, (F) Saline at 1 week after TBI, (G) Saline at 2 weeks after TBI, (H) Methamphetamine at 48 hours after TBI, (I) Methamphetamine at 1 week after TBI, (J) Methamphetamine at 2 weeks after TBI. 48 hours (Saline n=6; Methamphetamine n=6), 1 week (Saline n=5; Methamphetamine n=4), 2 week (Saline n=4; Methamphetamine n=4), * = $p<0.05$ compared to uninjured, *** = $p<0.001$; # = $p<0.05$ compared to 48 hour Saline, ### = $p<0.001$ compared to 48 hour Saline; ϕ = $p<0.05$ compared to 48 hour Methamphetamine, ϕϕϕ = $p<0.001$ compared to 48 hour Methamphetamine; scale bar = 80µm

In addition, we observed regions of autofluorescence in the ipsilateral corpus callosum at 48 hours post TBI (Figure 22A). The autofluorescence was detectable primarily in the green channel. Further scrutiny under high magnification showed a plethora of small anucleated cells that did not co-label with Iba1 (Figure 22B). Given their lack of nucleus, location and time after injury, we can be fairly confident that these were erythrocytes associated with hemorrhage caused by the severe TBI. Consistent with this theory, these erythrocytes were not seen at later time points. Furthermore, the general location of hemorrhages seen at 48 hours after injury corresponded with the areas of significant microglia activation seen at two weeks (Figure 21). Treatment with methamphetamine did not alter the appearance of hemorrhages seen 48 hours after injury.

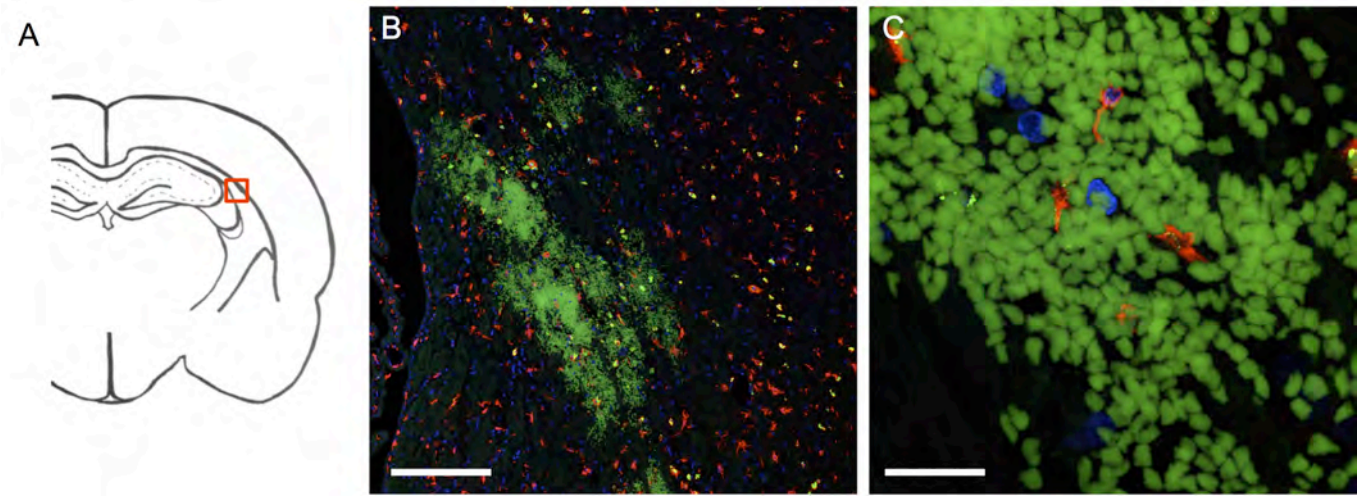

Figure 22: Hemorrhages are observed 48 hours after TBI. Images show the ipsilateral corpus callosum proximal to the cortical injury 48 hours after TBI labeled with Iba1 (red), CD68 (green) and DAPI (blue). (A) Schematic of a rat brain at Bregma -3.3 with red box marking location of analysis, (B) 10x of autofluorescent RBCs, scale bar = 200μm, (C) 60x image, scale bar = 20μm

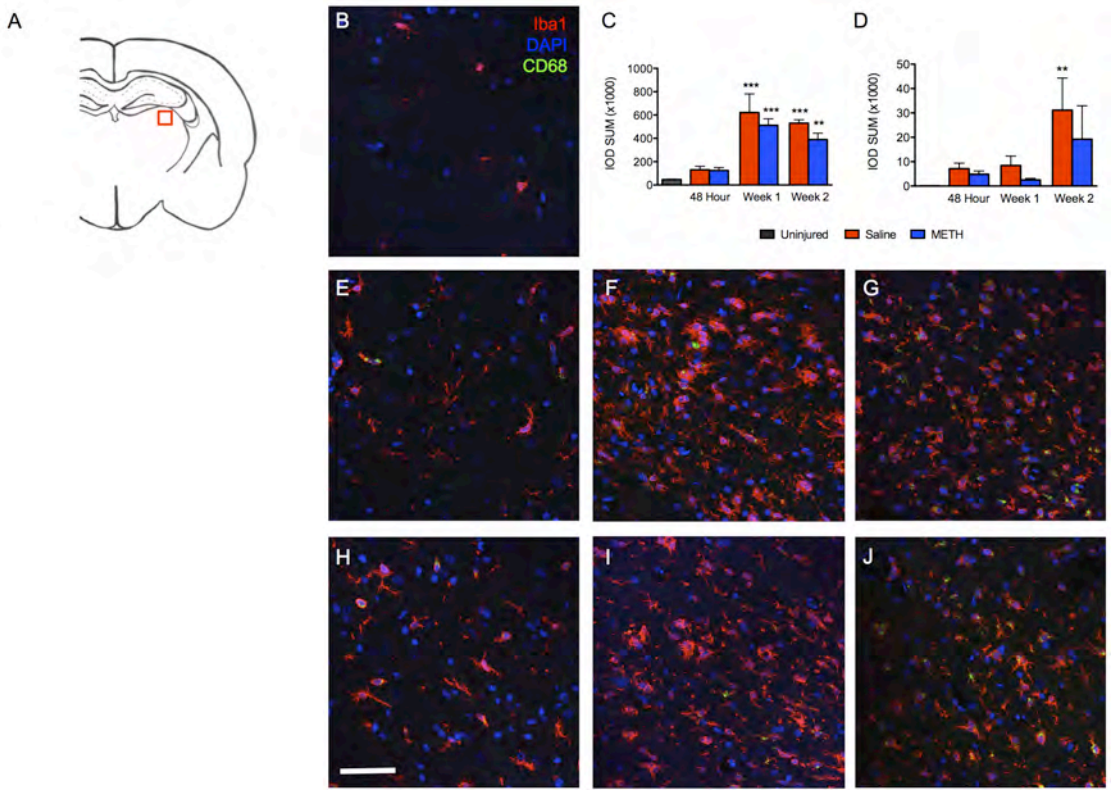

Figure 23: TBI causes a delayed increase of microglia within the ipsilateral laterodorsal thalamus. Images show the ipsilateral laterodorsal thalamic nuclei labeled with Iba1 (red), CD68 (green) and DAPI (blue). (A) Schematic of a rat brain at Bregma -3.3 with red box marking location of analysis, (B) Uninjured, (C) Summary graph of Iba1, (D) Summary graph of CD68, (E) Saline at 48 hours, (F) Saline 1 week after TBI, (G) Saline 2 weeks after TBI, (H) Methamphetamine at 48 hours post-TBI, (I) Methamphetamine one week post-TBI, and (J) Methamphetamine 2 weeks post-TBI. 48 hours (Saline n=6; Methamphetamine n=6), 1 Week (Saline n=5; Methamphetamine n=4), 2 Weeks (Saline n=4; Methamphetamine n=4), ** = p<0.01 compared to uninjured, *** = p<0.001 compared to uninjured; scale bar = 80μm

Activated microglia can be detected in the thalamus for up to one year post-TBI (Hernandez-Ontiveros, et al 2013; Acosta et al, 2014). Although unremarkable at 48 hours post-TBI, the laterodorsal thalamic nuclei displayed a very interesting response pattern at subsequent time points (Figure 23). By one-week post-TBI a significant increase of Iba1 was observed in both methamphetamine and saline treated animals. However, at two weeks post-TBI, while the prior high levels of Iba1 persisted, there was a significant increase of CD68 labeling. This suggests that although significant microglial activation occurred at both one and two weeks post-TBI within the laterodorsal thalamic nuclei, the activation phenotypes of microglia were changing. Our data showed the increase of microglia at one week was not associated with the increased phagocytic response seen at two weeks. Further studies are needed in order to investigate the function of the microglia responsible for the increase one-week post-TBI.

Granule neurons play a critical role in learning and memory. We have previously reported that methamphetamine treatment both increases neurogenesis of immature granule neurons and enhances learning and memory following severe TBI (XXXX). So in addition to microglia, we wanted to investigate the impact of methamphetamine on Mossy cells, are glutamatergic neurons within the hilus region of the hippocampus that provide extensive feed forward inhibition onto granule neurons through parvalbumin (PV) and somatostatin (SST) positive inhibitory interneurons (XXXX). We have recently reported that mossy cells also provide the first glutamatergic input onto developing granule neurons during adult neurogenesis (XXXX). Mossy cells thus play an important role in the functional maturation and migration of adult generated granule neurons. Mossy cells are exquisitely sensitive to loss following injury. Mossy cells also receive considerable catecholamine input. Given that methamphetamine causes an increased release of catecholamines, we hypothesized that methamphetamine treatment could result in the preservation of mossy cells and contribute to enhanced adult neurogenesis within the hippocampus. To investigate the hypothesis, we labeled mossy cells within paraffin embedded brain sections prepared from rats 48 hours after TBI. We compared uninjured controls with saline treated and methamphetamine treated rats (Figure 24).

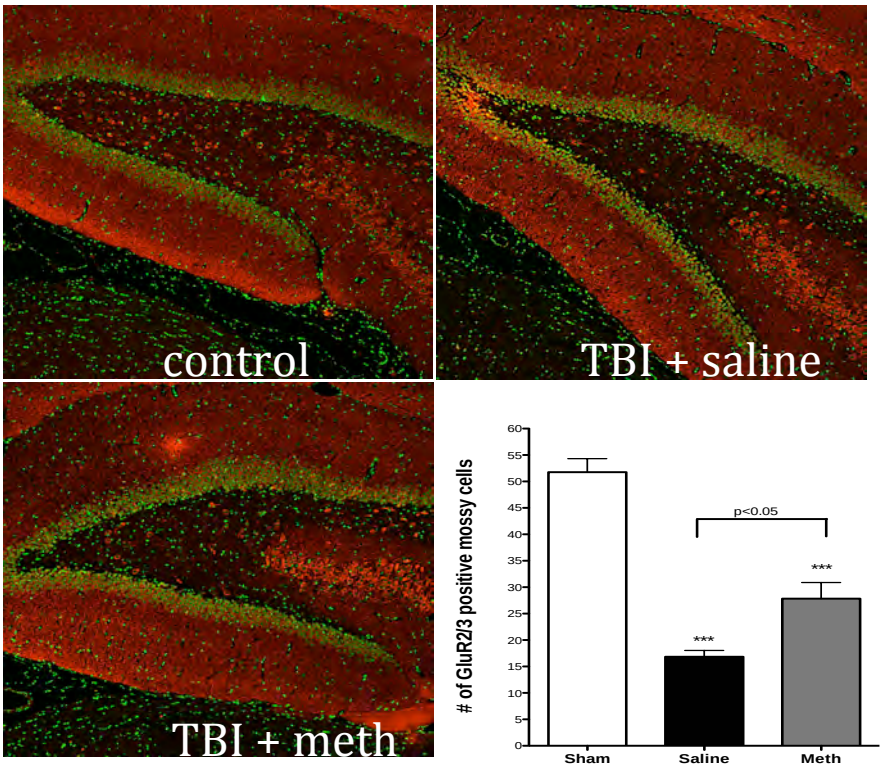

Figure 24. Methamphetamine treatment preserves mossy cells within the hippocampus hilar region. Paraffin embedded brain sections were stained with anti-GluR2/3 antibody (red) and neurotrace (green). ***=p<0.01

We observed a significant decrease in mossy numbers cells for both TBI groups (saline and methamphetamine treatment) compared to uninjured controls. However, there were significantly more mossy cells in methamphetamine treated rats compared to saline treated TBI controls. This data suggests that at 48 hours after injury (and 16 hours after methamphetamine infusion) methamphetamine caused a preservation of mossy cells.

We previously reported that TBI significantly reduced PV and SST positive inhibitory interneurons at 48 hours after TBI. This conclusion was based on a simple analysis of variance (ANOVA) comparison. We revisited this data and ran a multivariate analysis of variance (MANOVA) comparing the PV, SST and mossy cell data. Interestingly, MANOVA analysis confirmed that methamphetamine had no impact on PV positive cells. In contrast, MANOVA comparison indicated that methamphetamine had a significant impact on the preservation of both SST positive cells (p=0.003) and mossy cells (p=0.00002). A pairwise scatter plot of mossy cell and SST cell numbers confirmed a clear separation between the three treatment groups (Figure 25).

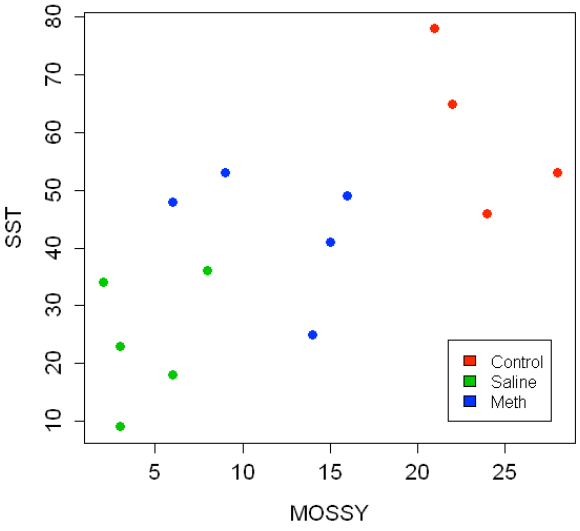

Figure 25. Pairwise comparison of mossy cell numbers with SST positive cell numbers. A treatment effect correlation was observed with the numbers of mossy cells and SST positive cells.

Conclusions

We have demonstrated that methamphetamine mediates neuroprotection in part, through dopamine dependent activation of D1 and D2 receptor and a PI3K/AKT signaling cascade. Aged rats and humans have reduced dopamine receptors. This may account for the reduction in methamphetamine efficacy in aged rats.

Unfortunately, female rats have a three-day estrous cycle. This means that they are exposed to the neuroprotective effects of progesterone and estrogen before, during and after injury. As a consequence, negative control, female rats that were exposed to saline recovered functional behavior that was similar to that observed in uninjured rats within about 2 weeks post injury (Figure 3). Thus, female rats offer a very poor model to examine a potential drug effect following sever TBI, as it is highly unlikely that we can improve a rats functional behavior beyond normal

We previously demonstrated that treatment with an IV bolus of 0.42 mg/kg followed by IV infusion with 0.05 mg/kg/hr for 24 hours produced increased white matter track remodeling at 5 and 6 weeks post injury in the CCI TBI model. The goal of this study was to test the hypothesis that increasing the dose to a bolus injection of 0.42 mg/kg followed by continuous IV infusion with 0.5 mg/kg/hr for 24 hours would increase the therapeutic effect. Our results suggest that there is not a dose dependent effect on methamphetamine mediated white matter track remodeling. We did also observe that methamphetamine enhances blood vessel labeling in the perilessional region. This data suggests that methamphetamine promotes angiogenesis.

We have further determined that methamphetamine induces increased microglia activation within the granular cell layer of the hippocampus. In addition, we have shown that methamphetamine treatment significantly preserves mossy cells and SST+ inhibitory interneurons within the dentate gyrus of the hippocampus after severe TBI. These drug-induced changes may contribute to the increased neurogenesis of granule neurons we previously reported (Rau et al., 2011).

Publications, Abstracts, and Presentations:

There have be no publications or presentations of this data within the past year.

Inventions, Patents and Licenses

International patent application no. PCT/US2007/076034 was filed on August 15, 2007, entitled: "METHOD OF REDUCING NEURONAL CELL DAMAGE". The application is directed to and claims methods of treating or reducing the occurrence of neuronal cell damage in a subject having a transient cerebral hypoxia and/or ischemic condition (e.g., stroke, traumatic brain injury) by administering a neuroprotective amount of methamphetamine to the subject within 16 hours after onset of the condition. National phase applications were filed and are pending in the following countries: Australia; Brazil; Canada; China; Europe; Hong Kong; India; Indonesia; Israel; Japan; Mexico; Philippines; Republic of Korea; Russian Federation; South Africa; and the United States. All applications claim priority to U.S. provisional application. no. 60/839,974, filed on August 23, 2006. Claims have now been awarded in the Belgium, Switzerland, Germany, Spain, France, Great Britain, Italy, Russia, Japan, Australia, and South African. Patent claims are about to be issued in Mexico and Philippines. The patent is still being prosecuted in the US.

Reportable Outcomes

The current studies suggest that we should limit participation in future clinical trials involving methamphetamine treatment of TBI to younger patients (perhaps less than 45 years of age). It seems a bit unnecessary to exclude females from future trials based on the current rat data. However, this may be a consideration.

References

Acosta SA, Tajiri N, Shinozuka K, Ishikawa H, Sanberg PR, Sanchez-Ramos J, Song S, Kaneko Y, Borlongan CV. 2014. Combination therapy of human umbilical cord blood cells and granulocyte colony stimulating factor reduces histopathological and motor impairments in an experimental model of chronic traumatic brain injury. PloS one 9:e90953.

Adnan A, Crawley A, Mikulis D, Moscovitch M, Colella B, Green R. 2013. Moderate-severe traumatic brain injury causes delayed loss of white matter integrity: evidence of fornix deterioration in the chronic stage of injury. Brain injury : [BI] 27:1415–22.

Bauer, J., Sminia, T., Wouterlood, F. G. and Dijkstra, C. D. 1994. Phagocytic activity of macrophages and microglial cells during the course of acute and chronic relapsing experimental autoimmune encephalomyelitis. Journal of neuroscience research 38: 365–375. Available from: 10.1002/jnr.490380402

Carson MJ, Doose JM, Melchior B, Schmid CD, Ploix CC. 2006. CNS immune privilege: hiding in plain sight. Immunological reviews [Internet] 213:48–65. Available from: http://onlinelibrary.wiley.com/resolve/openurl?genre=article&sid=nlm:pubmed&issn=0105-2896&date=2006&volume=213&spage=48

Chen Z, Jalabi W, Hu W, Park H-JJ, Gale JT, Kidd GJ, Bernatowicz R, Gossman ZC, Chen JT, Dutta R, Trapp BD. 2014. Microglial displacement of inhibitory synapses provides neuroprotection in the adult brain. Nature communications 5:4486.

Chung RS, Vickers JC, Chuah MI, West AK. 2003. Metallothionein-IIA promotes initial neurite elongation and postinjury reactive neurite growth and facilitates healing after focal cortical brain injury. The Journal of neuroscience : the official journal of the Society for Neuroscience 23:3336–42.

Ding GL, Chopp M, Poulsen DJ, Li L, Qu C, Li Q, Nejad-Davarani SP, Budaj JS, Wu H, Mahmood A, Jiang Q. 2013. MRI of neuronal recovery after low-dose methamphetamine treatment of traumatic brain injury in rats. PloS one [Internet] 8:e61241. Available from: http://dx.plos.org/10.1371/journal.pone.0061241

Glushakova O, Johnson D, Hayes R. 2014. Delayed Increases in Microvascular Pathology after Experimental Traumatic Brain Injury Are Associated with Prolonged Inflammation, Blood–Brain Barrier Disruption, and Progressive White Matter Damage. Journal of Neurotrauma 31:11801193

Hirko AC, Dallasen R, Jomura S, Xu Y. 2008. Modulation of inflammatory responses after global ischemia by transplanted umbilical cord matrix stem cells. Stem cells (Dayton, Ohio) 26:2893–901.

Hung C, Chen JW. 2012. Treatment of post-traumatic epilepsy. Current treatment options in neurology 14:293–306.

Rizzo F, Riboldi G, Salani S, Nizzardo M, Simone C, Corti S, Hedlund E. 2014. Cellular therapy to target neuroinflammation in amyotrophic lateral sclerosis. Cellular and molecular life sciences : CMLS 71:999–1015.

Gemma C, Bachstetter A. 2013. The role of microglia in adult hippocampal neurogenesis. Frontiers in Cellular Neuroscience 7.

Graeber MB & Mehraein P. 1994. Microglial rod cells. Neuropathology and applied neurobiology 20(2):178-80.

Hanisch U-KK. 2013. Functional diversity of microglia - how heterogeneous are they to begin with? Frontiers in cellular neuroscience [Internet] 7:65. Available from: http://dx.doi.org/10.3389/fncel.2013.00065

Hazra A, Macolino C, Elliott MB, Chin J. 2014. Delayed thalamic astrocytosis and disrupted sleep-wake patterns in a preclinical model of traumatic brain injury. Journal of neuroscience research 92:1434–45.

Hernandez-Ontiveros DG, Tajiri N, Acosta S, Giunta B, Tan J, Borlongan CV. 2013. Microglia activation as a biomarker for traumatic brain injury. Frontiers in neurology 4:30.

Kettenmann H, Kirchhoff F, Verkhratsky A. 2013. Microglia: new roles for the synaptic stripper. Neuron 77:10–8.

Kou Z, VandeVord PJ. 2014. Traumatic white matter injury and glial activation: from basic science to clinics. Glia 62:1831–55.

Kumar A, Loane DJ. 2012. Neuroinflammation after traumatic brain injury: opportunities for therapeutic intervention. Brain, behavior, and immunity 26:1191–201.

Loane DJ, Byrnes KR. 2010. Role of microglia in neurotrauma. Neurotherapeutics : the journal of the American Society for Experimental NeuroTherapeutics [Internet] 7:366–77. Available from: http://linkinghub.elsevier.com/retrieve/pii/S1933-7213(10)00088-7

Mehndiratta P, Sajatovic M. 2013. Treatments for patients with comorbid epilepsy and depression: a systematic literature review. Epilepsy & behavior : E&B [Internet] 28:36–40. Available from: http://linkinghub.elsevier.com/retrieve/pii/S1525-5050(13)00168-6

Peerzada H, Gandhi JA, Guimaraes AJ, Nosanchuk JD, Martinez LR. 2013. Methamphetamine administration modifies leukocyte proliferation and cytokine production in murine tissues. Immunobiology [Internet] 218:1063–8. Available from: http://linkinghub.elsevier.com/retrieve/pii/S0171-2985(13)00027-2

Perez-Polo JR, Rea HC, Johnson KM, Parsley MA, Unabia GC, Xu G, Infante SK, Dewitt DS, Hulsebosch CE. 2013. Inflammatory consequences in a rodent model of mild traumatic brain injury. Journal of neurotrauma [Internet] 30:727–40. Available from: http://www.liebertonline.com/doi/abs/10.1089/neu.2012.2650?url_ver=Z39.88-2003&rfr_id=ori:rid:crossref.org&rfr_dat=cr_pub%3dpubmed

Perry VH, Nicoll JA, Holmes C. 2010. Microglia in neurodegenerative disease. Nature reviews Neurology 6:193–201.

Raineri M, Gonzalez B, Goitia B, Garcia-Rill E, Krasnova IN, Cadet JL, Urbano FJ, Bisagno V. 2012. Modafinil abrogates methamphetamine-induced neuroinflammation and apoptotic effects in the mouse striatum. PloS one 7:e46599.

Rau TF, Kothiwal A, Zhang L, Ulatowski S, Jacobson S, Brooks DM, Cardozo-Pelaez F, Chopp M, Poulsen DJ. 2011. Low dose methamphetamine mediates neuroprotection through a PI3K-AKT pathway. Neuropharmacology 61:677–86.

Rau TF, Kothiwal AS, Rova AR, Brooks DM, Poulsen DJ. 2012. Treatment with low-dose methamphetamine improves behavioral and cognitive function after severe traumatic brain injury. The journal of trauma and acute care surgery 73:S165–72.

Rau TF, Kothiwal AS, Rova AR, Brooks DM, Rhoderick JF, Poulsen AJ, Hutchinson J, Poulsen DJ. 2014. Administration of low dose methamphetamine 12 h after a severe traumatic brain injury prevents neurological dysfunction and cognitive impairment in rats. Experimental neurology 253:31–40.

Sternberger NH, Sternberger LA. 1987. Blood-brain barrier protein recognized by monoclonal antibody. Proceedings of the National Academy of Sciences of the United States of America 84:8169–73.

Su P, Zhang J, Zhao F, Aschner M, Chen J, Luo W. 2014. The interaction between microglia and neural stem/precursor cells. Brain research bulletin 109C:32–38.

Taylor SE, Morganti-Kossmann C, Lifshitz J, Ziebell JM. 2014. Rod microglia: a morphological definition. PloS one 9:e97096.

Thomas D. 2004. Methamphetamine Neurotoxicity in Dopamine Nerve Endings of the Striatum Is Associated with Microglial Activation. Journal of Pharmacology and Experimental Therapeutics 311.

Tiesman HM, Konda S, Bell JL. 2011. The epidemiology of fatal occupational traumatic brain injury in the U.S. American journal of preventive medicine [Internet] 41:61–7. Available from: http://linkinghub.elsevier.com/retrieve/pii/S0749-3797(11)00200-5

Trifilieff P, Feng B, Urizar E, Winiger V, Ward RD, Taylor KM, Martinez D, Moore H, Balsam PD, Simpson EH, Javitch JA. 2013. Increasing dopamine D2 receptor expression in the adult nucleus accumbens enhances motivation. Molecular psychiatry (9):1025-33. Available from: 10.1038/mp.2013.57.

Walker KR, Tesco G. 2013. Molecular mechanisms of cognitive dysfunction following traumatic brain injury. Frontiers in aging neuroscience [Internet] 5:29. Available from: http://dx.doi.org/10.3389/fnagi.2013.00029

Wang G, Zhang J, Hu X, Zhang L, Mao L, Jiang X, Liou AK, Leak RK, Gao Y, Chen J. 2013. Microglia/macrophage polarization dynamics in white matter after traumatic brain injury. Journal of cerebral blood flow and metabolism : official journal of the International Society of Cerebral Blood Flow and Metabolism 33:1864–74.

Wang T, Huang X-JJ, Van KC, Went GT, Nguyen JT, Lyeth BG. 2013. Amantadine Improves Cognitive Outcome and Increases Neuronal Survival after Fluid Percussion Traumatic Brain Injury in Rats. Journal of neurotrauma [Internet]. Available from: http://www.liebertonline.com/doi/abs/10.1089/neu.2013.2917?url_ver=Z39.88-2003&rfr_id=ori:rid:crossref.org&rfr_dat=cr_pub%3dpubmed

Xiong Y, Mahmood A, Chopp M. 2013. Animal models of traumatic brain injury. Nature reviews Neuroscience [Internet] 14:128–42. Available from: http://dx.doi.org/10.1038/nrn3407

Ziebell JM, Taylor SE, Cao T, Harrison JL, Lifshitz J. 2012. Rod microglia: elongation, alignment, and coupling to form trains across the somatosensory cortex after experimental diffuse brain injury. Journal of neuroinflammation 9:247.